# INTERNAL AND INTERFACE SHEAR STRENGTHS OF GEOSYNTHETIC CLAY LINERS

The attached keynote paper from the 3rd International Symposium on Geosynthetic Clay Liners presents recent research on internal and interface shear strengths of GCLs. Key aspects of this research include static and dynamic shear strengths, as well as the role of shear displacement rate. The data suggests that internal GCL shear strengths are affected by product type, normal stress, and shear displacement rate. For textured geomembrane/GCL interfaces, the failure mode depends on both the normal stress and displacement rate. For the needlepunch reinforced GCLs tested in this study (Bentomat DN), GCL internal failure only occurred in interface tests performed at extremely high normal stresses: 28,800 psf (partial internal failure) and 43,200 psf.

Interestingly, tests run at lower shear displacement rates did not necessarily yield conservative shear strength values. These results suggest that the current shear displacement rate recommendations (0.04 inch/min for geomembrane/GCL interface tests, and 0.004 inch/min for hydrated GCL internal tests) may need to be re-evaluated.



800.527.9948 Fax 847.577.5566

# Internal and Interface Shear Strengths of Geosynthetic Clay Liners

P. J. Fox. Department of Structural Engineering, University of California-San Diego, La Jolla, California, USA. pjfox@ucsd.edu

ABSTRACT
This paper presents a survey of recent research on the internal and interface shear strengths of geosynthetic clay liners (GCLs). Essential concepts of shear strength testing and stress–displacement behavior are reviewed, followed by detailed discussions of GCL internal and interface shear strengths measured for static and dynamic loading conditions. North American research is emphasized and test results focus primarily on needle-punched GCLs and textured geomembrane products. In general, the data indicate the significance of normal stress level and shear displacement rate on failure mode and shear strength of GCLs and GCL interfaces.

## 1. INTRODUCTION

Internal and interface shear strengths of geosynthetic clay liners (GCLs) are needed for static and seismic stability analyses in the design of waste containment facilities and other facilities that incorporate these materials as hydraulic barriers. These strengths are given particular attention because bentonite, the essential component of a GCL, is a very weak material after hydration and thus can provide a potential surface for shear failure. Reported values of GCL internal and interface shear strengths show significant variability due to variability in component materials and manufacturing processes, differences in testing equipment and procedures, and changes in the design, manufacture and application of GCLs over time. As a result, it has long been recognized that design shear strength parameters for GCLs and other geosynthetics must be obtained using product-specific and project-specific tests (Koerner et al. 1986, Bove 1990, Eith et al. 1991, Sabatini et al. 2002). Current understanding of the shear strengths of GCLs and GCL interfaces is still evolving and recent research has been conducted on issues such as dynamic shear strength and shear strength under high normal stress conditions.

This paper presents a survey of recent research on internal and interface shear strengths for GCLs. Essential concepts of shear strength testing and shear stress–displacement behavior are presented, as well as data on static and dynamic shear strength of hydrated GCLs and GCL interfaces. Conclusions are drawn with regard to GCL shear strength behavior for common GCL and GCL interface materials, with emphasis on needle-punched (NP) GCLs and textured geomembrane (GMX) products. A complete presentation and interpretation of available test data on the peak, large displacement and residual shear strengths of GCLs and GCL interfaces is beyond the scope of this paper. Chiu and Fox (2004) present findings from a large database of unpublished and published test data that has been compiled on the internal and interface shear strengths of unreinforced and NP GCLs. Zornberg et al. (2005) and McCartney et al. (2009) also present findings from a large database of GCL internal and interface shear strengths. Other sources of good quality shear strength data include Gilbert et al. (1996), Fox et al. (1998a), Thiel et al. (2001), Triplett and Fox (2001), Fox and Stark (2004) and Nye and Fox (2007).

## 2. TEST METHODS

A substantive review of test methods for the measurement of GCL shear strength is provided by Fox and Stark (2004). The primary conclusions of this work are:

- Direct shear is expected to remain the preferred general test method for GCL shear strength because it can be used for any type of GCL product, a large range of normal stress is possible, large specimens can be tested, post-peak response can be obtained and shear strengths are measured in one direction with nominally uniform shear displacement.

- Specimen gripping surfaces should be rigid, provide good drainage and prevent slippage of the test specimen. Slippage will likely cause progressive failure of the specimen and, as a result, yield conservative peak shear strengths and unconservative large displacement shear strengths. Fox and Kim (2008) provide a detailed analysis of this effect.
- Although multi-interface shear tests can reduce the amount of testing required and provide a better simulation of field conditions, such tests are more difficult to perform and interpret than single-interface tests and are generally not recommended at the current time.
- It is important to select the proper normal stress range for GCL shear tests because failure envelopes are commonly nonlinear and because the normal stress level can affect the failure mode of a test specimen. The normal stress during hydration and consolidation may also affect measured GCL shear strength and should generally follow the sequence expected in the field.
- GCL specimens should be fully hydrated under the normal stress expected in the field at the time of hydration. After hydration, a GCL specimen should be consolidated to the shearing normal stress (if necessary) using small load increments to minimize bentonite extrusion.
- A maximum shear displacement rate $R$ = 0.1 mm/min. is recommended for static internal shear tests of hydrated GCLs, whereas a maximum $R$ = 1 mm/min. is recommended for dry GCLs and GCL interfaces. Recent data presented in this paper and elsewhere may lead to a re-evaluation of these recommendations.
- Failed test specimens should be inspected carefully after shearing to assess the surface(s) on which failure occurred and the general nature of the failure. Wrinkling, necking or tearing of the supporting geosynthetics indicates that a shear test may need to be repeated with improved gripping surfaces.
- Good quality shear testing will generally produce smooth shear stress–displacement relationships that display close similarity and do not contain double peaks or large undulations. Shear stress–displacement relationships should always be examined to make a preliminary assessment of the quality of GCL shear test results.

## 3. SHEAR STRESS-DISPLACEMENT BEHAVIOR

### 3.1 Shear Stress-Displacement Relationships

Shear stress–displacement relationships for GCLs and GCL interfaces, as obtained from short-term shear tests, are used to determine shear strength parameters and to conduct stability analyses that yield estimates of displacement. Shear stress–displacement relationships can also provide an important indication of test data quality. Figure 1 shows a typical relationship between shear stress ($\tau$) and shear displacement ($\Delta$) for a hydrated GCL specimen at constant shearing normal stress ($\sigma_{n,s}$). Shear stress increases rapidly to a peak shear strength ($\tau_p$) at the beginning of the test. The corresponding displace-

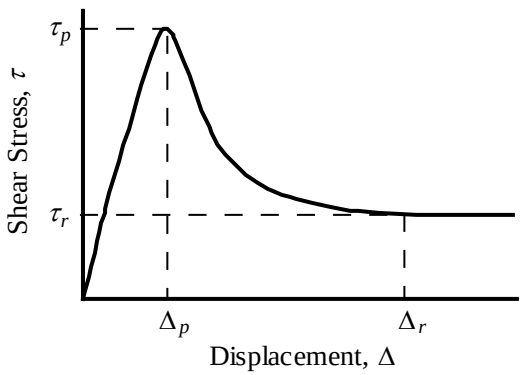


Figure 1. Typical shear stress–displacement relationship for internal shear test of a hydrated GCL specimen (Fox and Stark 2004).

ment at peak ($\Delta_p$) is usually, but not always, less than 50 mm. In general, values of $\Delta_p$ are smallest for unreinforced GCLs, larger for NP GCLs and largest for stitch-bonded (SB) GCLs. As displacement continues, all GCLs and most GCL interfaces experience post-peak strength reduction, in which measured shear stress decreases and ultimately reaches a residual shear strength ($\tau_r$) after which no further strength reduction occurs with continued displacement. The displacement associated with the residual strength ($\Delta_r$) may be as large as 0.1 to 0.5 m or more, depending on the material(s) tested and the normal stress level. Residual shear conditions are best determined by plotting $\tau$ vs. log $\Delta$ to more clearly distinguish changes in $\tau$ (or the lack thereof) at large $\Delta$ (Stark 1997). In cases where $\tau_r$ is not measured, a "large displacement" shear strength ($\tau_{ld}$) is often reported along with the displacement at which it was measured (e.g., a common notation is $\tau_{75mm}$ or $\tau_{75}$ for the shear strength at $\Delta$ = 75 mm).

Post-peak strength reduction can result from several mechanisms, including clay particle reorientation at the failure surface, volume increase of material within the shear zone (e.g., soil), loss of roughness for interface geosynthetic materials (e.g., GMX) and failure of reinforcement or supporting geotextiles. Internal shear failure of NP GCLs generally occurs as the reinforcement fibers rupture and/or pull out of the geotextiles, whereas SB GCLs fail as the reinforcing stitches rupture or tear out of the geotextiles. The residual strength ratio ($\tau_r / \tau_p$) for internal shear of GCLs varies widely, with reported values as low as 0.04, depending on the product type, hydration condition and normal stress level. In general, $\tau_r / \tau_p$ values increase in the following order: hydrated NP GCL < hydrated SB GCL < hydrated unreinforced GCL < dry unreinforced GMS-supported GCL < dry unreinforced GMX-supported GCL (Fox et al. 1998a, Chiu and Fox 2004). The term "dry" denotes a GCL specimen that was tested in the as-received moisture condition.

### 3.2 Unreinforced GCLs

Two examples of shear stress–shear displacement ($\tau - \Delta$) relationships for internal shear of unreinforced GCLs, as obtained from direct shear tests, are shown in Figure 2(a). The first relationship was obtained for a dry unreinforced GCL consisting of bentonite encapsulated between two high-density polyethylene (HDPE) GMXs and glued to the lower GMX ($\sigma_{n,s}$ = 96 kPa, specimen size = 300 × 300 mm, $R$ = 1 mm/min.). The second relationship was obtained for an unreinforced woven/woven (W/W) geotextile (GT)-supported GCL sheared in the fully hydrated condition ($\sigma_{n,s}$ = 72 kPa, specimen size = 406 × 1067 mm, $R$ = 0.1 mm/min.). The hydrated unreinforced GCL has low peak shear strength and $\tau_r / \tau_p$ = 0.4. Hydrated unreinforced GCLs are not appropriate for applications on slopes or applications on flat ground in which shear stresses are transferred from nearby slopes (Stark et al. 1998). The dry encapsulated GCL has much higher peak and residual shear strengths and a large displacement strength ratio of $\tau_{60} / \tau_p$ = 0.81, indicating that significantly less post-peak strength reduction occurs in the dry condition. The high residual shear strength of dry GCLs is advantageous for designs in which the GCL is sheared beyond the peak. Values of $\Delta_p$ are relatively small (< 10 mm) for both unreinforced GCLs.

### 3.3 Reinforced GCLs

Needle-punched or stitched reinforcement is used to transmit shear stress across the weak bentonite layer of a hydrated GCL, with the needle-punched variety now being the more common choice. The additional confinement provided by needle-punched fibers also decreases the water content of the hydrated bentonite and the potential for bentonite migration, although significant migration has been observed under severe loading conditions (Fox et al. 1996, Fox et al. 1998b, Stark 1998, Fox et al. 2000). The peel strength test (ASTM D 6496) is routinely used as a quality control index test in the manufacturing of NP GCLs to assess the relative strength and density of fiber reinforcement.

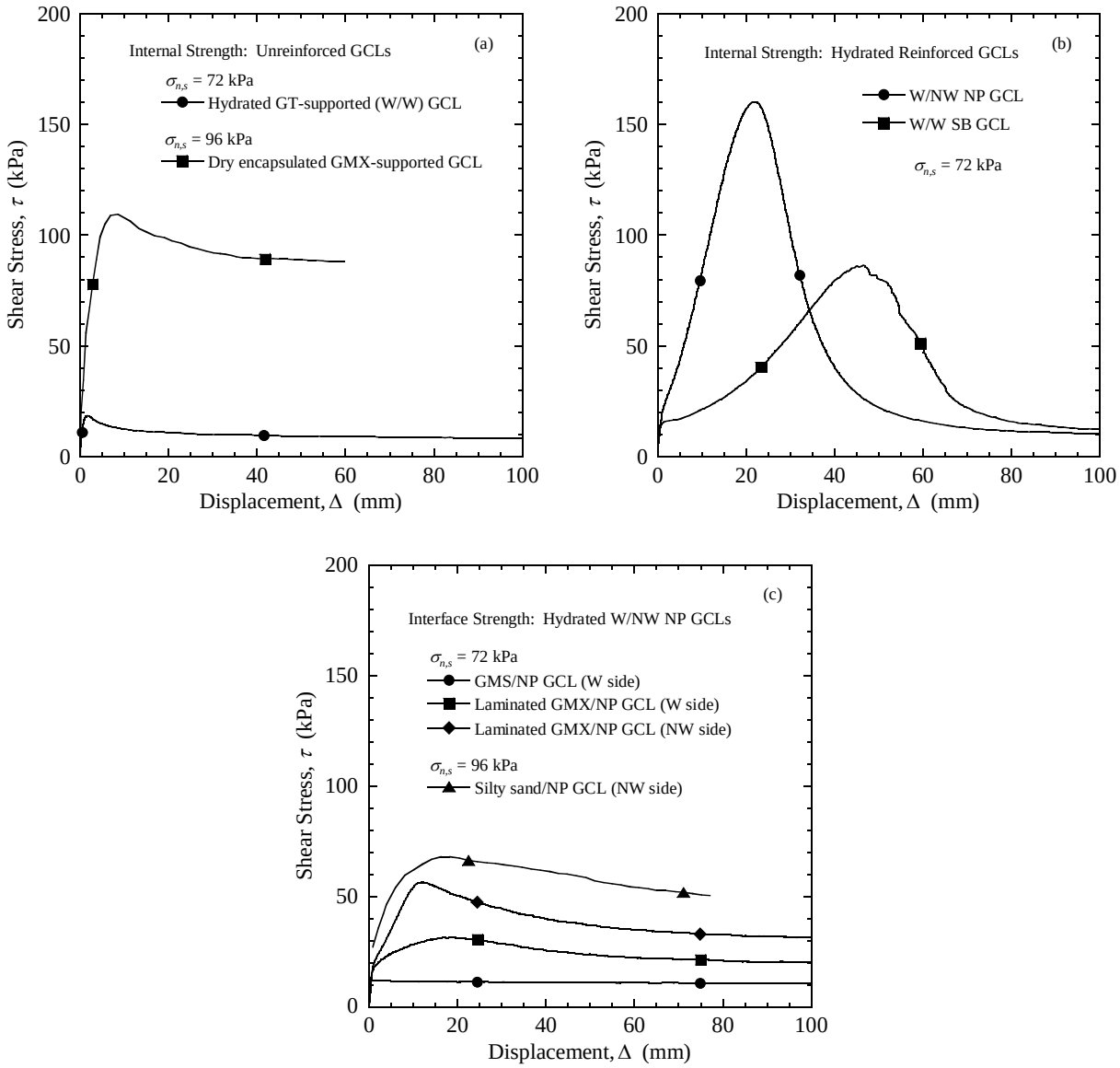


Figure 2. Examples of shear stress–displacement relationships for: (a) unreinforced GCLs, (b) hydrated reinforced GCLs and (c) hydrated NP GCL interfaces (Fox and Stark 2004).

Figure 2(b) shows examples of $\tau - \Delta$ relationships for internal shear of a hydrated woven/nonwoven (W/NW) NP GCL and a hydrated W/W SB GCL ($\sigma_{n,s}$ = 72 kPa, specimen size = 406 × 1067 mm, $R$ = 0.1 mm/min.). These relationships display higher peak shear strengths than the hydrated unreinforced GCL in Fig. 2(a) due to additional shear resistance provided by the geosynthetic reinforcement and lower residual strength ratios ($\tau_r / \tau_p$ = 0.06 and 0.11 for NP and SB, respectively) due to failure of the reinforcement. At this normal stress level, the SB GCL has a peak strength that is approximately one-half that of the NP GCL. The value of $\tau_r / \tau_p$ for internal strength of hydrated NP GCLs can be as low as 0.04 (Fox et al. 1998a), indicating that reinforced GCLs can experience very large strength reduction if the peak strength is exceeded. Dry NP GCLs can also experience large post-peak strength reductions at low normal stress (Feki et al. 1997). In Figure 2(b), the SB GCL has a $\Delta_p$ value that is approximately twice that of the NP GCL. This is due to the ability of the supporting geotextiles to stretch around the lines of stitching prior to tearing of the geotextiles at the stitching (see Fuller 1995 for photograph of this

effect). The essentially uniform reinforcement density of a NP GCL prevents this type of deformation, resulting in a lower $\Delta_p$ value.

### 3.4 Reinforced GCL Interfaces

Shear stress–displacement relationships for four NP GCL interfaces are shown in Figure 2(c). Three tests were performed with HDPE geomembranes and one was performed with silty sand. All peak interface strengths are smaller and all large-displacement strengths are larger than for the internal GCL shear tests shown in Fig. 2(b). The relationship for the GMS/NP GCL interface has the lowest $\tau_p$, the highest residual strength ratio ($\tau_r / \tau_p$ = 0.82) and is nearly independent of whether the W or NW side of the NP GCL is tested (Triplett and Fox 2001). As shown in Figure 2(c), this independence does not hold for GMX/NP GCL interfaces. Peak and residual interface shear strengths for a GMX sheared against the NW side of a NP GCL are generally higher than those corresponding to the W side. von Maubeuge and Eberle (1998) also found that GMX/NP GCL (NW side) interfaces had higher shear strengths when the NP GCL was manufactured using a thicker NW GT. Differences in GM texturing process (e.g., laminated vs. coextruded) have a relatively minor effect on GMX/GCL interface shear strength (Chiu and Fox 2004). Post-peak strength reductions are higher for GMX interfaces than for GMS interfaces due to higher levels of damage that occur during shear. Large displacement strength ratios for the GMX interfaces in Figure 2(c) are higher for the W side ($\tau_{200} / \tau_p$ = 0.57) than for the NW side ($\tau_{200} / \tau_p$ = 0.47). Although less published information is available, $\tau - \Delta$ relationships for soil/GCL interfaces show considerable variability, depending on the soil type and method of preparation/compaction (Chiu and Fox 2004). The silty sand/NP GCL relationship in Figure 2(c) has moderate post-peak strength reduction ($\tau_{77} / \tau_p$ = 0.74). Little to no post-peak strength reduction has been observed for shear tests conducted on dry sand/NP GCL interfaces (Garcin et al. 1995) and moist silty sand/SB GCL interfaces (Feki et al. 1997). Values of $\Delta_p$ for the GCL interfaces shown in Figure 2(c) are all less than 20 mm. In general, $\Delta_p$ values for most NP GCL interfaces are less than those for internal shear of NP GCLs (Chiu and Fox 2004).

## 4. GCL INTERNAL SHEAR STRENGTH

### 4.1 Static Shear Strength of Unreinforced GCLs

The drained shear strength of hydrated sodium bentonite is the lowest of any natural soil (Mesri and Olson 1970). Figure 3 shows peak and residual failure envelopes obtained from torsional ring shear tests of a hydrated unreinforced GM-supported GCL conducted by Dr. T. Stark (University of Illinois, USA). The peak and residual friction angles are approximately $\phi_p$ = 8º and $\phi_r$ = 5º, respectively. Fox et al. (1998a) measured similarly low friction angles ($\phi_p$ = 10.2º and $\phi_r$ = 4.7º) for a hydrated unreinforced GT-supported GCL (see Figure 4). These values of $\phi_r$ are in good agreement with the value of 4.0º measured from ring shear tests on sodium montmorillonite (Müller-Vonmoos and Løken 1989).

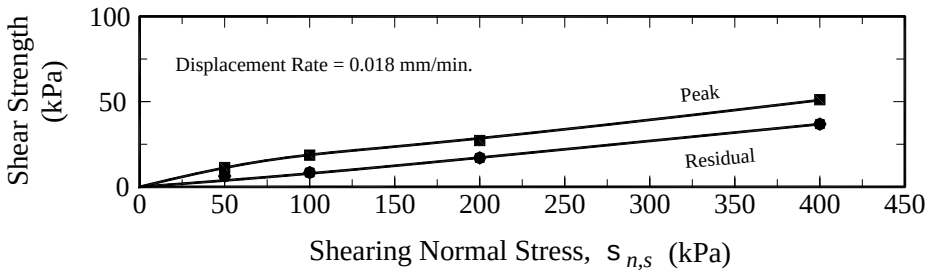


Figure 3. Peak and residual failure envelopes for a hydrated unreinforced GM-supported GCL (Fox and Stark 2004).

Encapsulating unreinforced bentonite between two geomembranes will significantly reduce the amount of bentonite hydration, resulting in higher shear strength and lower susceptibility for bentonite migration (Stark 1998, Thiel et al. 2001). Chiu and Fox (2004) showed that dry unreinforced GMX-supported GCLs generally have slightly lower internal peak strengths and much higher residual strengths than hydrated NP GCLs. The main design issue for unreinforced encapsulated GCLs thus becomes the amount of bentonite hydration that is expected, on average, as a result of liquid transmission through perforations, defects and seam overlaps in the encapsulating geomembranes (diffusion of water vapor through the intact geomembrane is expected to be negligible). Lateral moisture flow along GM wrinkles may also contribute to bentonite hydration (Cowland 1997). Thiel et al. (2001) and Giroud et al. (2002) presented theoretical analyses of long-term hydration of encapsulated bentonite for GM-supported GCLs. For landfill liner systems with 300 mm GM overlaps, Thiel et al. (2001) calculated that approximately 10 to 35 percent of the encapsulated bentonite will become hydrated over a design period of 250 years, depending on the moisture condition of the subgrade. Stability analyses for such a system are then conducted using prorated peak and residual strength envelopes based on the estimated ratio of dry and hydrated areas for the encapsulated GCL.

## 4.2 Static Shear Strength of Reinforced GCLs

Geosynthetic reinforcement greatly increases the peak shear strength of hydrated GCLs. Figure 4 shows peak and residual failure envelopes for a W/W SB GCL and two W/NW NP GCLs. The NP GCL specimens were taken from two rolls of the same commercial product having peel strengths ($F_p$) of 85 N/10 cm and 160 N/10 cm. Corresponding failure envelopes for a hydrated unreinforced W/W GCL are also shown for comparison. Each failure envelope is modestly nonlinear. A linear envelope was also fitted between the endpoints of each nonlinear envelope. The unreinforced GCL has the lowest peak strength at any normal stress and the linear failure envelope can be characterized by $c_p$ = 2.4 kPa and $\phi_p$ = 10.2º. The peak shear strength of the SB GCL increases slightly with normal stress for $\sigma_{n,s}$ < 72 kPa and is nearly constant at 91 kPa for $\sigma_{n,s}$ > 72 kPa. The peak shear strength of the NP GCL increases sharply with $\sigma_{n,s}$ and shows good correlation with peel strength. Values of shear strength parameters (linear envelope) for the 85 N product are $c_p$ = 42.3 kPa and $\phi_p$ = 41.9º, whereas values for the 160 N product are $c_p$ = 98.2 kPa and $\phi_p$ = 32.6º. This finding is generally consistent with the work of Heerten et al. (1995) and von Maubeuge and Eberle (1998), in which internal stability of NP GCLs for a given slope angle and soil cover depth was directly related to peel strength. The residual failure envelope for each GCL product in Figure 4 is independent of reinforcement type and essentially equal to that of hydrated bentonite ($c_r$ = 1.0 kPa, $\phi_r$ = 4.7º). Thus, the residual shear strength of hydrated GCLs can only be improved by increasing the residual shear strength of the hydrated bentonite. Some researchers have tried to accomplish this by incorporating a granular admixture into the bentonite layer (Schmitt et al. 1997, Fox 1998). The practicality of maintaining a sufficiently uniform mixing process on a production scale, such that GCL hydraulic conductivity remains uniformly low, is however doubtful.

In the Fox et al. (1998a) study, the contribution of stitched reinforcement to peak strength of the SB GCL was found to be essentially independent of $\sigma_{n,s}$ and solely dependent on the tearing strength of the woven geotextiles. Thus, the increase of $\tau_p$ with $\sigma_{n,s}$ for the SB GCL (Figure 4) was due to increased shear strength of the bentonite/W GT interface. The contribution of needle-punched reinforcement to peak strength of the NP GCL increased almost linearly with $\sigma_{n,s}$ and displayed a clear correlation with peel strength. This suggests that the needle-punched fiber connections for an NP GCL are frictional in nature.

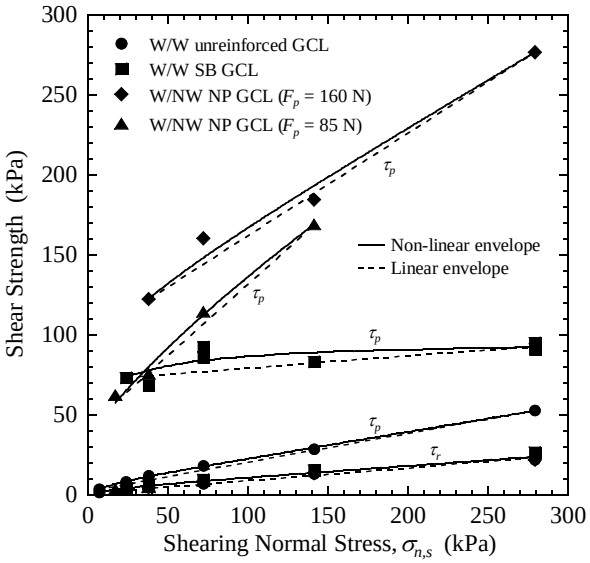


Figure 4. Peak and residual failure envelopes for hydrated unreinforced, stitch-bonded and needle-punched GCLs (Fox et al. 1998a).

### 4.3 Dynamic Shear Strength of Reinforced GCLs

Geosynthetic liner systems are occasionally subjected to earthquakes and other dynamic loads. As such, the characterization of the dynamic shear behavior of these materials is important for prediction of long-term performance. Lai et al. (1998) conducted the first study on the effects of cyclic loading on the shear strength of GCLs. They reported static and cyclic strengths of dry and hydrated specimens (dia. = 80 mm) of an unreinforced GM-supported GCL in direct simple shear. The dry product showed no strength reduction, and even a slight strength increase due to bentonite densification, under cyclic loading. When hydrated, GCL shear strength decreased under cyclic loading. Similar to natural soils, the number of cycles needed to reach failure decreased with increasing cyclic stress ratio (cyclic shear stress amplitude/static peak shear strength).

A multi-year experimental program is currently in progress to investigate the dynamic shear strength of NP GCLs and NP GCL interfaces. All tests have been performed using a large dynamic direct shear machine that is shown in Figure 5 and described in detail by Fox et al. (2006). The main features of this machine include large specimen size (305 × 1067 mm), large normal stress range ($\sigma_{n,s}$ = 0 to 2000 kPa), large maximum shear displacement (254 mm), large range of displacement rate ($R$ = 0.01 to 30,000 mm/min), negligible machine friction and the capability to measure specimen volume change. A GCL specimen is sheared between the underside of a horizontal pullout plate and the floor of the test chamber, each of which is covered with an aggressive gripping surface (modified truss plates). The gripping surfaces permit drainage of the specimen on both sides and are sufficiently rough that end-clamping of the geosynthetics is not required. This allows a specimen to fail along the weakest surface and avoids possible progressive failure effects. The shearing system is powered by a 245 kN hydraulic actuator that can impart bidirectional (i.e., back-and-forth) motion to the pullout plate. The maximum frequency for sinusoidal loading with a displacement amplitude of 25 mm is 4 Hz. Normal stress is provided by two bellowed air bladders that rest on an overlying stationary load plate. Between the load plate and the pullout plate, a layer of 517 free-rolling stainless steel balls reduce the shear stress due to friction to 0.27% of the applied normal stress. Vertical displacement of the load plate due to specimen volume change is continuously monitored during hydration and shearing using a LVDT. GCL specimens are hydrated from a water reservoir at the rear of the machine through a network of drainage channels in both shearing surfaces. The system has an automated digital servocontroller that provides full control over machine operation and data collection. Using this machine, Nye and Fox (2007) presented an extensive testing program of monotonic and cyclic direct shear tests on a needle-punched GCL at a single normal stress level (141 kPa). The primary findings from this work are that the dynamic shear

strength generally increases with increasing displacement rate for monotonic (i.e., single direction) shear tests and that displacement amplitude is the main parameter controlling shear response during and after cyclic shear tests.

Figure 5. Dynamic direct shear machine (Fox et al. 2006).

Direct shear tests have been recently conducted to measure the rapid internal shear response of a W/NW NP GCL (Fox et al. 2009). The average peel strength of the material is 1580 N/m (ASTM D 6496). Specimens were hydrated using the two-stage procedure described by Fox et al. (1998a), in which each specimen is pre-hydrated to the expected final water content prior to placing in the shear machine. Following hydration, 68 GCL specimens were subjected to displacement-controlled monotonic shear tests to evaluate the effect of shear displacement rate $R$ on peak and residual shear strengths and displacements at peak strength. Tests were performed at four normal stress levels ($\sigma_{n,s}$ = 141, 348, 692 and 1382 kPa) with displacement rates ranging from 0.1 to 28,000 mm/min., the latter of which is the maximum limit of the machine for these loads. Figure 6 shows representative $\tau - \Delta$ relationships obtained for $\sigma_{n,s}$ = 348 kPa. The slowest rate (0.1 mm/min) is the recommended value for conventional static shear testing (Fox and Stark 2004). The curves are generally similar in shape with well-defined peak and residual shear strengths. Large post-peak strength reduction occurs for each $R$ value due to failure of the reinforcement. Although peak and residual shear strengths show some rate dependency, the general similarity of curves in Figure 6 suggests that the basic mechanism of failure is consistent for all displacement rates.

Values of $\tau_p$ are shown in Figure 7(a) for each normal stress as a function of $R$. As expected, peak strengths increase with increasing normal stress at each displacement rate. At $\sigma_{n,s}$ = 141 kPa, a static peak shear strength of 158 kPa was measured for $R$ = 0.1 mm/min. As $R$ increased, the average $\tau_p$ value increased to 185 kPa at $R$ = 1000 mm/min. and then decreased to 153 kPa at $R$ = 28,000 mm/min. Thus, peak strength increased to a maximum of 17% above the static value and then returned to approximately the same value at the highest displacement rate. Tests conducted at $\sigma_{n,s}$ = 348 kPa yielded a generally similar response. At this normal stress level, the highest peak strength (266 kPa) occurred at $R$ = 100 to 1000 mm/min. and was 13% higher than the static strength (236 kPa). At $R$ = 28,000 mm/min., the peak strength (250 kPa) was 6% higher than the static shear strength. For $\sigma_{n,s}$ = 692 kPa, peak strengths increased 14.5% from 352 kPa at $R$ = 0.1 mm/min. to 403 kPa at $R$ = 10,000 mm/min. and then decreased only slightly thereafter. Peak shear strengths at the highest normal stress level (1382 kPa) again increased with increasing displacement rate. In this case, $\tau_p$ reached the highest value (499 kPa) at $R$ = 1,000 mm/min., which was 23% above the static strength of 404 kPa. Beyond 1,000 mm/min., $\tau_p$ decreased to approximately 469 kPa. At some stress levels (e.g., 1382 kPa) the data display significant scatter, which is attributed to variability of needle-punched reinforcement. The

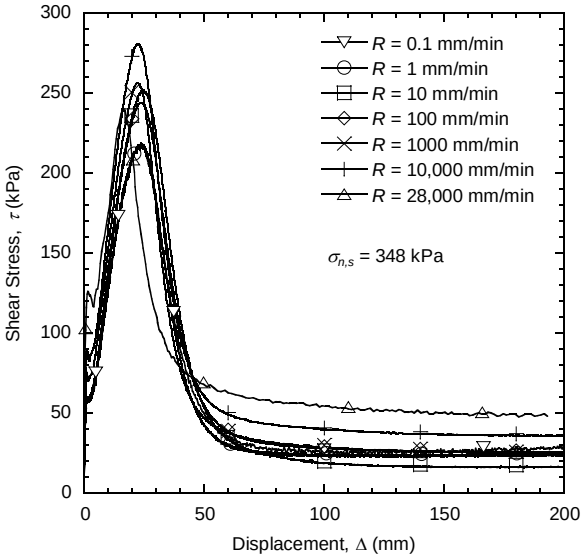


Figure 6. Shear stress-displacement relationships for seven monotonic shear tests of a hydrated W/NW NP GCL (Fox et al. 2009).

observed trend in peak strengths suggests an increasing and then decreasing resistance of reinforcing fibers as $R$ increases. Zornberg et al. (2005) found that $\tau_p$ decreased as $R$ increased from 0.0015 to 1 mm/min. at high normal stress ($\sigma_{n,s}$ = 520 kPa). The slower shear data in Figure 7(a) are inconclusive with regard to this point (also see discussion by Fox 2006). A key observation with regard to Figure 7(a) is that, in general, static peak strengths obtained at 0.1 mm/min. are conservative at each normal stress level.

Corresponding displacements at peak shear strength $\Delta_p$ are shown in Figure 7(b). At each displacement rate, the value of $\Delta_p$ decreased with increasing normal stress. The data for static shear ($R$ = 0.1 mm/min) are somewhat contradictory to the findings of Fox et al. (1998a) in which $\Delta_p$ for the same GCL product ranged from 21 to 26 mm and did not show a clear trend when $\sigma_{n,s}$ was increased from 38 to 279 kPa. Figure 7(b) also shows that, at each normal stress, $\Delta_p$ generally decreased with increasing $R$. At $\sigma_{n,s}$ = 141 kPa, $\Delta_p$ decreased from approximately 31 mm at the slow rates to 21 mm at the fastest rate. Corresponding decreases for the other three normal stresses were 27 mm to 16 mm for $\sigma_{n,s}$ = 348 kPa, 19 mm to 15 mm for $\sigma_{n,s}$ = 692 kPa, and 16 mm to 13 mm for $\sigma_{n,s}$ = 1382 kPa. The explanation for this effect may be that, at higher $R$, the initially loaded reinforcing fibers fail more quickly because there is less time available for load transfer to nearby fibers. If correct, it is interesting that this effect generally produces higher peak shear strengths (Figure 7(a)).

Residual shear strengths $\tau_r$ obtained from the same monotonic tests are shown in Figure 7(c). As expected, residual strengths also increased with increasing normal stress at each displacement rate. At each normal stress, $\tau_r$ values increased with increasing $R$ for $R \geq 1$ mm/min, which is consistent with most previous studies (e.g., Fox et al. 1998a, Eid et al. 1999). This increase is particularly marked for $R$ > 1000 mm/min. However, the reverse trend is observed for $R$ < 1 mm/min and becomes pronounced at the highest normal stress. A general increase in residual strength with increasing $R$ has been attributed to rate-dependent shear resistance of the hydrated bentonite (Fox et al. 1998a). The data in Figure 7(c) indicate that the static shear displacement rate of 0.1 mm/min. may produce unconservative residual strengths for some dynamic applications and that lower values of $\tau_r$ can be obtained at $R$ = 1 mm/min.

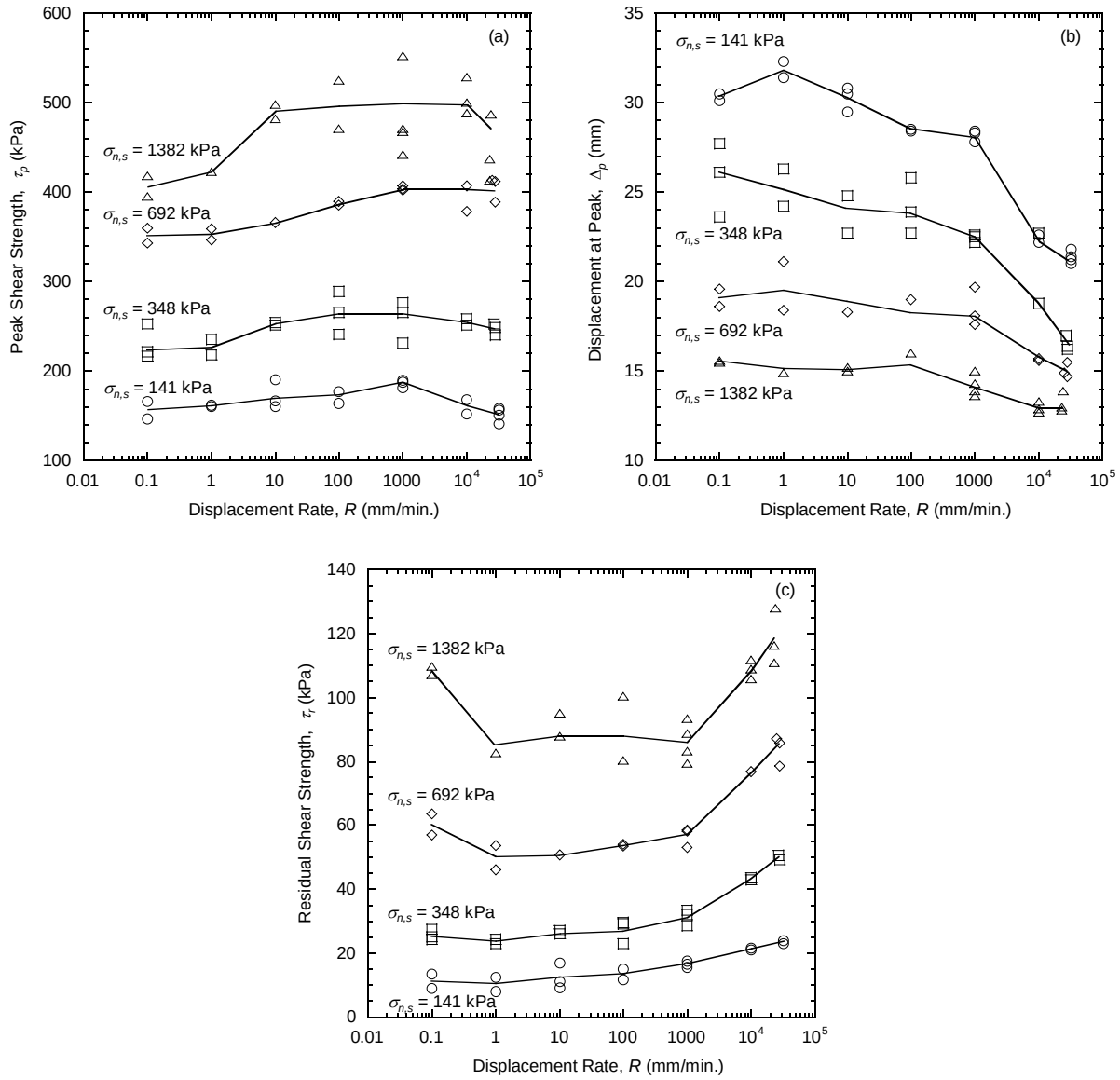


Figure 7. Effect of displacement rate on: (a) peak shear strength, (b) displacement at peak shear strength and (c) residual shear strength for a hydrated W/NW NP GCL (Fox et al. 2009).

## 5. GMX/GCL INTERFACE SHEAR STRENGTH

### 5.1 Static Interface Shear Strength of Reinforced GCLs

Recent data has been obtained using the dynamic shear machine (Figure 5) for static ($R$ = 0.1 mm/min.) interface shear strength of a hydrated GMX/NP GCL interface for a large range of normal stress. The NW/NW NP GCL had no thermal bonding and an average peel strength of 2170 N/m. The HDPE GMX had single-sided structured texturing, a density of 0.94 g/cm$^3$ and a thickness of 1.5 mm (60 mils). The average asperity (i.e., spike) height was 0.72 mm (29 mils) and the spacing of asperities was 5.3 mm in the machine direction and 5.5 mm in the transverse direction.

Peak and large displacement failure envelopes for the GMX/GCL interface are shown in Figure 8, along with corresponding envelopes from internal shear tests of the GCL itself. Solid lines were obtained using regression and indicate consistent failure modes, whereas dashed lines indicate changing failure mode between data points. GCL specimens yielded higher peak shear strengths than GMX/GCL specimens at

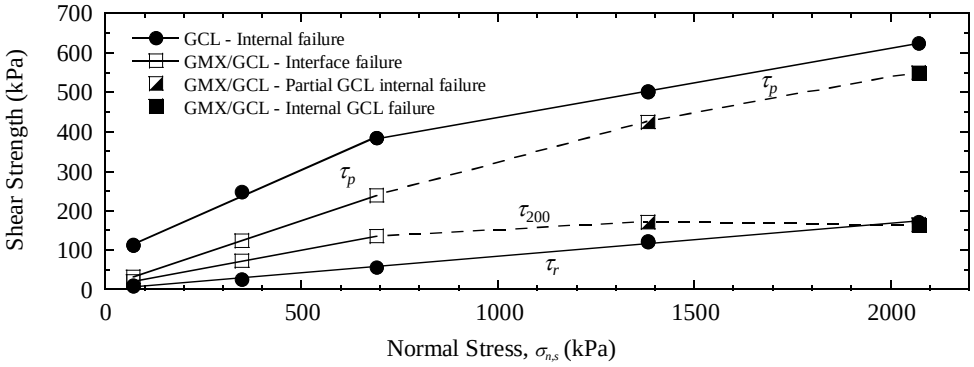


Figure 8. Peak and large displacement failure envelopes for NW/NW NP GCL internal and GMX/NP GCL interface shear tests.

all normal stress levels. Peak failure envelopes for both test series are nonlinear and indicate a friction angle that decreases with increasing normal stress. The peak failure envelope for GCL internal shear is well described as bi-linear using the following regression equations:

$\tau_p$ = 83.7 kPa + $\sigma_{n,s}$ tan 23.7° ($71.9 \leq \sigma_{n,s} \leq 692$ kPa) [1]

$\tau_p$ = 261.2 kPa + $\sigma_{n,s}$ tan 9.9° ($692 \leq \sigma_{n,s} \leq 2071$ kPa) [2]

The linear portion of the GMX/GCL peak failure envelope corresponds to interface failure and is described by:

$\tau_p$ = 8.2 kPa + $\sigma_{n,s}$ tan 18.4° ($71.9 \leq \sigma_{n,s} \leq 692$ kPa) [3]

At higher normal stress levels, changes in GMX/GCL failure mode may be responsible for the nonlinearity exhibited in the peak failure envelope.

The residual strength failure envelope for the GCL internal shear tests is linear over the entire stress range and essentially passes through the origin. The regression equation is:

$\tau_r$ = 1.3 kPa + $\sigma_{n,s}$ tan 4.8° ($71.9 \leq \sigma_{n,s} \leq 2071$ kPa) [4]

The secant residual friction angle (i.e., envelope passing through the origin) for this data is also 4.8°. A residual friction angle of 4.8° is consistent with published data for different types of GCLs obtained using direct shear tests (Fox et al. 1998a, Nye and Fox 2007) and for sodium montmorillonite obtained using ring shear tests (Müller-Vonmoos and Løken 1989). At low normal stress levels, the GMX/GCL specimens failed at the interface and yielded higher large displacement (200 mm) strengths than the GCL specimens. The corresponding linear envelope is described by:

$\tau_{200}$ = 7.3 kPa + $\sigma_{n,s}$ tan 10.5° ($71.9 \leq \sigma_{n,s} \leq 692$ kPa) [5]

As normal stress increased, the GMX/GCL failure mode transitioned to internal GCL shear and the $\tau_{200}$ failure envelope becomes nonlinear, actually sloping downward slightly to merge with the GCL $\tau_r$ envelope at $\sigma_{n,s}$ = 2071 kPa. Figure 8 provides an important example illustrating that data extrapolation to lower or higher normal stress levels based on the assumption of a linear failure envelope may significantly overestimate available peak or large displacement shear strengths and should not be attempted for these types of geosynthetic materials. The only exception is the residual internal shear strength of the hydrated GCL, which produced a linear envelope over the entire normal stress range.

## 5.2 Dynamic Interface Shear Strength of Reinforced GCLs

An experimental program was recently completed on GMX/NP GCL dynamic interface shear strength for the same geosynthetic materials as described in Sec. 4.1. Using the dynamic shear machine, twenty-nine displacement-controlled monotonic interface shear tests were conducted at five levels of shearing normal stress ($\sigma_{n,s}$ = 13, 348, 692, 1382 and 2071 kPa) and shear displacement rates $R$ ranging from 0.1 to 29,000 mm/min. The normal stress range was sufficiently large to include conditions typical of cover systems and bottom liner systems of very deep (150 m) landfills.

Figure 9 shows $\tau - \Delta$ relationships that were measured for the highest normal stress level ($\sigma_{n,s}$ = 2071 kPa). In each case, shear stress quickly rises to $\tau_p$ and then decreases to a substantially lower large-displacement shear strength $\tau_{200}$. Interestingly, the failure mode changes with displacement rate for these tests. Failure occurred internal to the GCL for $R$ = 0.1 and 1 mm/min., partially internal to the GCL and partially at the GMX/GCL interface for $R$ = 100 mm/min., and at the GMX/GCL interface for $R$ = 10,000 and 16,000 mm/min. Specimens with complete internal GCL failures reached a residual shear condition, whereas shear strength for the specimens with partial internal and interface failures was still decreasing at $\Delta$ = 200 mm.

Figure 10(a) shows a plot of $\tau_p$ versus $R$ for the GMX/GCL shear tests at all normal stress levels. Tests conducted at $\sigma_{n,s}$ = 13, 348 and 692 kPa produced interface failures for all displacement rates. At $\sigma_{n,s}$ = 1382 kPa, partial GCL internal failures occurred for $R$ = 0.1, 1 and 100 mm/min., with slower rates yielding larger internal failure percentages, and interface failures occurred for $R$ = 10,000 and 25,000 mm/min. The failures at $\sigma_{n,s}$ = 2071 kPa are discussed above. The data clearly indicate that, above a certain threshold normal stress, failure mode depends on both normal stress and displacement rate. Internal failures occurred at high normal stress and low displacement rates. As normal stress decreased or displacement rate increased, the failure mode transitioned to interface failure. Thus, shear displacement rate had a major influence on failure mode for these materials at high normal stress and may be generally more significant in this regard than previously considered.

Peak shear strength increased substantially with increasing displacement rate for $\sigma_{n,s}$ = 13 kPa ($\tau_p$ = 7.75 kPa at 1 mm/min., $\tau_p$ = 26.5 kPa at 29,000 mm/min.) and was essentially independent of $R$ for $\sigma_{n,s}$ = 348, 692 and 1382 kPa. Values of $\tau_p$ also increased with increasing rate for $\sigma_{n,s}$ = 2071 kPa, which is related to the transition in failure mode. Nye and Fox (2007) and Fox et al. (2009) found that

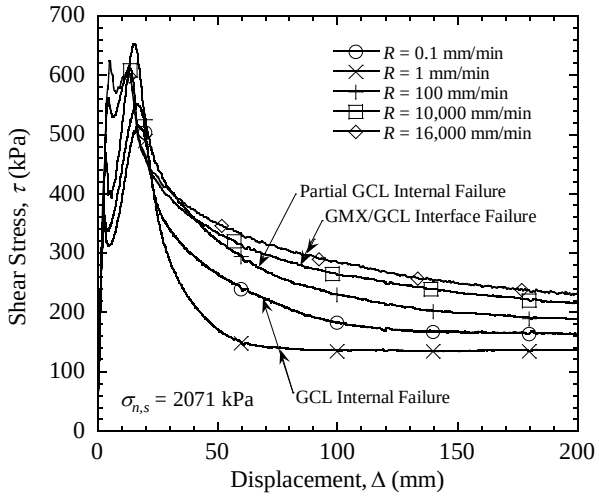


Figure 9. Shear stress-displacement relationships for GMX/NP GCL monotonic shear tests for $\sigma_{n,s}$ = 2071 kPa and varying displacement rates (Ross et al. 2010).

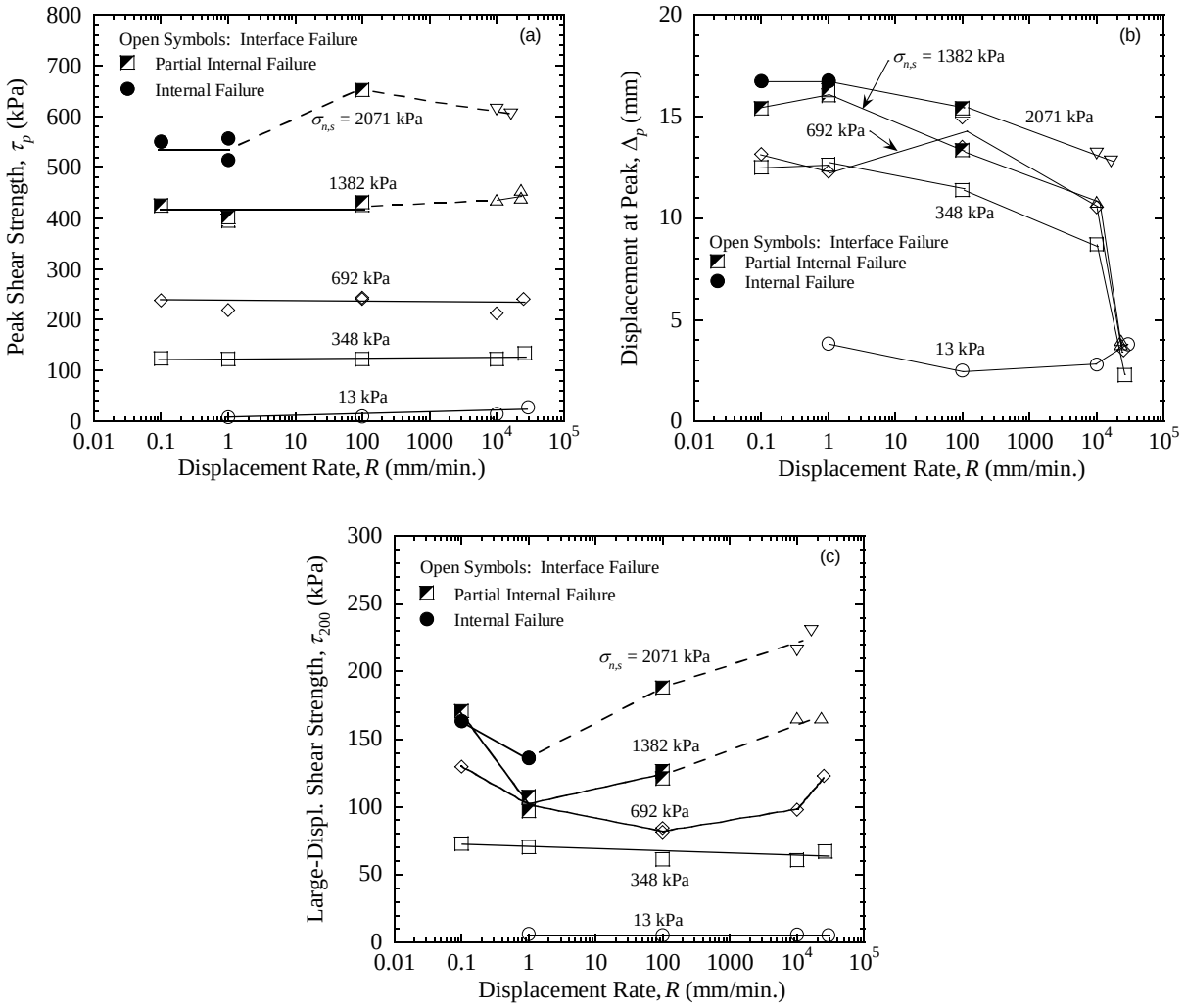


Figure 10. Effect of displacement rate on: (a) peak shear strength, (b) displacement at peak shear strength, and (c) large displacement shear strength for a hydrated GMX/NP GCL interface (Ross et al. 2010).

internal shear strength of NP GCLs generally increases with increasing displacement rate, which could explain the failure mode transition observed at the higher normal stress levels in Figure 10(a).

Figure 10(b) shows a corresponding plot of displacements at peak shear strength $\Delta_p$. At the lowest normal stress (13 kPa), values of $\Delta_p$ were relatively constant and ranged from 2 to 4 mm. The other tests at higher normal stress levels display different behavior. In general, $\Delta_p$ decreased with increasing displacement rate and, for $R \leq$ 10,000 mm/min., ranged from 9 to 17 mm. At the fastest displacement rate, however, $\Delta_p$ decreased sharply to 2-4 mm, except at $\sigma_{n,s}$ = 2071 kPa. Figure 10(b) also shows that $\Delta_p$ generally increased with increasing normal stress at each displacement rate. This trend is opposite to that observed for GCL internal shear strength tests in Figure 7(b).

Figure 10(c) presents $\tau_{200}$ versus $R$. Displacement rate had little effect on large-displacement strengths for $\sigma_{n,s}$ = 13 and 348 kPa. However, a decreasing and then increasing trend is observed for $\sigma_{n,s}$ = 692, 1382 and 2071 kPa. The trend for $\sigma_{n,s}$ = 692 kPa is not related to failure mode and may be

due to pore pressure conditions on the failure surface. The trends at $\sigma_{n,s}$ = 1382 and 2071 kPa likely reflect a combination of pore pressure effects and differing failure modes. A GCL internal failure will generally have a lower large-displacement shear strength than a GMX/GCL interface failure (Triplett and Fox 2001, Chiu and Fox 2004). Thus, the partial or complete GCL internal failures produced relatively low values of $\tau_{200}$ at high normal stress in Figure 10(c).

The above data has potential ramifications for the recommended displacement rate for GMX/GCL static shear tests at high normal stress. Recommended displacement rates for internal and interface static shear tests of GCLs are 0.1 and 1 mm/min., respectively (Fox and Stark 2004). A slower rate was recommended for internal shear tests to allow more time for dissipation of possible shear-induced excess pore pressures from the failure surface. On the other hand, the GMX/GCL interface tests of Triplett and Fox (2001) did not show a clear displacement rate effect and 1 mm/min. was considered reasonable. Figure 10 clearly indicates that displacement rate effects are more complex than previously considered and, as such, recommended values for static shear tests of GMX/GCL interfaces may need to be re-evaluated.

## 6. CONCLUSIONS

This paper presents a survey of recent research on the internal and interface shear strengths of geosynthetic clay liners (GCLs). North American research is emphasized and test results focus primarily on needle-punched (NP) GCLs and textured geomembrane (GMX) products. The data show interesting trends and indicate that internal GCL shear strengths are affected by product type, normal stress and shear displacement rate. For GMX/GCL interfaces, failure mode depends on both normal stress and displacement rate. Interestingly, peak shear strengths measured at the static displacement rate of 0.1 mm/min. were generally conservative at each normal stress level for both internal and interface shear tests. However, large displacement/residual shear strengths measured at higher rates (e.g., 1 mm/min.) were often lower than static values. The significance of these data is that displacement rate effects are more complex than previously considered. This may require the re-evaluation of recommended displacement rates for static shear tests conducted at high normal stress levels.

## ACKNOWLEDGEMENTS

This research was supported in part by the U.S. National Science Foundation and several grants from CETCO (Hoffman Estates, Illinois, USA). The following individuals also contributed greatly to this research effort by conducting shear tests during their graduate studies: Jason Ross, Michael Rowland, John Scheithe and Joseph Sura. Contributions from Jim Olsta of CETCO and Dr. Timothy Stark of the University of Illinois and his students are also gratefully acknowledged.

## REFERENCES

ASTM D 6496. Standard Test Method for Determining Average Bonding Peel Strength Between the Top and Bottom Layers of Needle-Punched Geosynthetic Clay Liners, *ASTM International*, West Conshohocken, Pennsylvania, USA.

Bove, J.A. (1990). Direct shear friction testing for geosynthetics in waste containment, *Geosynthetic Testing for Waste Containment Applications*, STP 1081, Koerner, R.M., editor, ASTM International, West Conshohocken, Pennsylvania, USA, 241-256.

Chiu, P., and Fox, P.J. (2004). Internal and interface shear strengths of unreinforced and needle-punched geosynthetic clay liners, *Geosynthetics International*, 11(3): 176-199.

Cowland, J.W. (1997). A design perspective on shear strength testing of geosynthetic clay liners, *Testing and Acceptance Criteria for Geosynthetic Clay Liners*, STP 1308, Well, L.W., editor, ASTM International, West Conshohocken, Pennsylvania, USA, 229-239.

Eid, H.T., Stark, T.D., and Doerfler, C.K. (1999). Effect of shear displacement rate on internal shear strength of a reinforced geosynthetic clay liner, *Geosynthetics International*, 6(3): 219-239.

Eith, A.W., Boschuk, J., and Koerner, R.M. (1991). Prefabricated bentonite clay liners, *Geotextiles and Geomembranes*, 10(5-6): 575-599.

Feki, N., Garcin, P., Faure, Y.H., Gourc, J.P., and Berroir, G. (1997). Shear strength of geosynthetic clay liner systems, *Geosynthetics '97,* IFAI, Long Beach, California, USA, 2: 899-912.

Fox, P.J. (1998). Research on geosynthetic clay liners at Purdue University, *Geotechnical News*, 16(1): 35-40.

Fox, P.J. (2006). Discussion of "Analysis of a large database of GCL internal shear strength results" by Zornberg, J.G., McCartney, J.S., and Swan, R.H., Jr., *Journal of Geotechnical and Geoenvironmental Engineering*, 132(10): 1373-1375.

Fox, P.J., and Stark, T.D. (2004). State-of-the-art report: GCL shear strength and its measurement, *Geosynthetics International*, 11(3): 141-175.

Fox, P.J., and Kim, R.H. (2008). Effect of progressive failure on measured shear strength of geomembrane/GCL interface, *Journal of Geotechnical and Geoenvironmental Engineering*, 134(4): 459-469.

Fox, P.J., De Battista, D.J., and Chen, S.H. (1996). Bearing capacity of geosynthetic clay liners for cover soils of varying particle size, *Geosynthetics International*, 3(4): 447-461.

Fox, P.J., De Battista, D.J., and Mast, D.G. (2000). Hydraulic performance of geosynthetic clay liners under gravel cover soils, *Geotextiles and Geomembranes*, 18(2-4): 179-201.

Fox, P.J., Rowland, M.G., and Scheithe, J.R. (1998a). Internal shear strength of three geosynthetic clay liners, *Journal of Geotechnical and Geoenvironmental Engineering*, 124(10): 933-944.

Fox, P.J., Triplett, E.J., Kim, R.H., and Olsta, J.T. (1998b). Field study of installation damage for geosynthetic clay liners, *Geosynthetics International*, 5(5): 491-520.

Fox, P.J., Nye, C.J., Morrison, T.C., Hunter, J.G., and Olsta, J.T. (2006). Large dynamic direct shear machine for geosynthetic clay liners, *Geotechnical Testing Journal*, 29(5): 392-400.

Fox, P.J., Sura, J.M., Ross, J.D., and Olsta, J.T. (2009). Rapid shear response of a needle-punched GCL*, Geosynthetics '09*, Salt Lake City, Utah, USA, 386-391.

Fuller, J.M. (1995). Landfill cap designs using geosynthetic clay liners, *Geosynthetic Clay Liners*, Koerner, R.M., Gartung, E., and Zanzinger, H., editors, Balkema, Rotterdam, The Netherlands, 129-140.

Garcin, P., Faure, Y.H., Gourc, J.P., and Purwanto, E. (1995). Behavior of geosynthetic clay liner (GCL): Laboratory tests*, 5th International Symposium on Landfills*, Cagliari, Italy, 1: 347-358.

Gilbert, R.B., Fernandez, F., and Horsfield, D.W. (1996). Shear strength of reinforced geosynthetic clay liner, *Journal of Geotechnical Engineering*, 122(4): 259-266.

Giroud, J.P., Thiel, R.S., Kavazanjian, E., and Lauro, F.J. (2002). Hydrated area of a bentonite layer encapsulated between two geomembranes, *7th International Conference on Geosynthetics*, Nice, France, 2: 827-832.

Heerten, G., Saathoff, F., Scheu, C., and von Maubeuge, K.P. (1995). On the long-term shear behavior of geosynthetic clay liners (GCLs) in capping sealing systems, *Geosynthetic Clay Liners,* Koerner, R.M., Gartung, E., and Zanzinger, H., editors, Balkema, Rotterdam, The Netherlands, 141-150.

Koerner, R.M., Martin, J.P., and Koerner, G.R. (1986). Shear strength parameters between geomembranes and cohesive soils, *Geotextiles and Geomembranes*, 4(1): 21-30.

Lai, J., Daniel, D.E., and Wright, S.G. (1998). Effects of cyclic loading on internal shear strength of unreinforced geosynthetic clay liner, *Journal of Geotechnical and Geoenvironmental Engineering*, 124(1): 45-52.

McCartney, J.S., Zornberg, J.G., Swan, R.H., Jr. (2009). Analysis of a large database of GCL-geomembrane interface shear strength results, *Journal of Geotechnical and Geoenvironmental Engineering*, 135(2): 209-223.

Mesri, G., and Olson, R.E. (1970). Shear strength of montmorillonite, *Geotechnique*, 20(3): 261-270.

Müller-Vonmoos, M., and Løken, T. (1989). The shearing behavior of clays, *Applied Clay Science*, 4(2): 125-141.

Nye, C.J., and Fox, P.J. (2007). Dynamic shear behavior of a needle-punched geosynthetic clay liner, *Journal of Geotechnical and Geoenvironmental Engineering*, 133(8): 973-983.

Ross, J.D., Fox, P.J., and Olsta, J.T. (2010). Dynamic shear testing of a geomembrane/geosynthetic clay liner interface*, 9th International Conference on Geosynthetics*, Guaruja, Brazil, in press.

Sabatini, P.J., Griffin, L.M., Bonaparte, R., Espinoza, R.D., and Giroud, J.P. (2002). Reliability of state of practice for selection of shear strength parameters for waste containment system stability analyses, *Geotextiles and Geomembranes*, 20(4): 241-262.

Schmitt, K.E., Bowders, J.J., Gilbert, R.B., and Daniel, D.E. (1997). Enhanced shear strength of sodium bentonite using frictional additives, *International Containment Technology Conference*, St. Petersburg, Florida, USA, 355-361.

Stark, T.D. (1997). Effect of swell pressure on GCL cover stability, *Testing and Acceptance Criteria for Geosynthetic Clay Liners*, STP 1308, Well, L.W., editor, ASTM International, West Conshohocken, Pennsylvania, USA, 30-44.

Stark, T.D. (1998). Bentonite migration in geosynthetic clay liners, *6th International Conference on Geosynthetics,* IFAI, Atlanta, Georgia, USA, 1: 315-320.

Stark, T.D., Arellano, D., Evans, W.D., Wilson, V.L., and Gonda, J.P. (1998). Unreinforced geosynthetic clay liner case history, *Geosynthetics International*, 5(5): 521-544.

Thiel, R., Daniel, D.E., Erickson, R.B., Kavazanjian, E., Jr., and Giroud, J.P. (2001). *The GSE GundSeal GCL Design Manual*, GSE Lining Technologies, Inc., Houston, Tex.

Triplett, E.J., and Fox, P.J. (2001). Shear strength of HDPE geomembrane/geosynthetic clay liner interfaces, *Journal of Geotechnical and Geoenvironmental Engineering*, 127(6): 543-552.

von Maubeuge, K.P., and Eberle, M.A. (1998). Can geosynthetic clay liners be used on slopes to achieve long-term stability?, *3rd International Congress on Environmental Geotechnics*, Lisbon, Portugal, 1: 375-380.

Zornberg, J.G., McCartney, J.S., and Swan, R.H., Jr. (2005). Analysis of a large database of GCL internal shear strength results, *Journal of Geotechnical and Geoenvironmental Engineering*, 131(3): 367-380.